# CRACK INITIATION AND GROWTH IN CIRCULAR SAW MADE FROM TOOL STEEL

**İsmail UCUN, Mehmet ÇOLAKOĞLU, Süleyman TAŞGETİREN**

Afyon Kocatepe University, Faculty of Technical Education, Department of Mechanics, Afyonkarahisar, Turkey.

## ABSTRACT

Fatigue of the circular saw made from tool steel and used in metal industry to cut especially metal bars and pipes is investigated in this study. Due to having small tooth root radius, the circular saw is much more risky to get crack damage at tooth root region. Radial and tangential forces are also effective at this region for fatigue crack initiation. In high cutting speed and feed rate of the circular saw, higher stress concentration particularly occurs at that region. To examine the fatigue and failure in the circular saw, specimens used in experiment are prepared from the damaged circular saw and are subjected to different mechanical tests. In the theoretical study, stress and fracture behaviours of the saw are determined by finite element method. Results and reasons of the failure are assessed.

**Keywords:** Circular saw, Crack, Finite element analysis, Failure analysis, Tool steel.

## 1. INTRODUCTION

Circular saw manufactured from tool steel is mostly used to cut profile cross-sectioned materials in metal industry. Feed rate and revolution speed (rpm) of the disk, type of material being cut, etc. are important parameters for failure of the disk. Varied forces occur during the cutting process in the circular saw. When the disk starts to get dull, these forces are getting bigger [1]. As a result of this, undesired damage occurs at the tooth root region. The saw material is as important as feed rate and cutting speed for wearing and damaging. Therefore, recent studies are especially focused to develop better materials and on processing for the saw to protect it from damage [2].

Fukaura et al.[3] investigated the fatigue properties of two types of cold-work steels tempered at various temperatures. The S-N curves of the steels were similar to those of most structural steels. The results showed that the subsurface fatigue cracks initiation was dominant at lower alternating stresses. Yesildal et al.[4] determined the fatigue characteristics of the hot work tool steel X40CrMoV 51 at high temperatures. In the experiment, cylindrical specimens were used at the temperature rage between 50-600$^o$C. As a result, the fatigue limit of the material at room temperature was determined as 432 MPa but it decreased to 383 MPa at 400 $^o$C and also it stayed constant between 400-600$^o$C.

The aim of this study is to analyze the fatigue cracking of a circular saw encountered in a real application. In the analysis, stress and fracture behaviors were determined by using finite element method. The classical cutting machine and circular saw used to cut profile cross-sectioned metals are shown in Figure 1. Fig. 1 also gives the typical crack propagation in a circular saw. The dimensions of saw and saw teeth are given in Figure 2. The mechanical behavior of the disk is investigated on specimens, prepared from tooth root region of the disk, subjected to varied mechanical tests. It is found that cracks under different loads grow at tooth root regions of the circular saw since it has small tooth root radius which causes much higher stress concentration in this area.

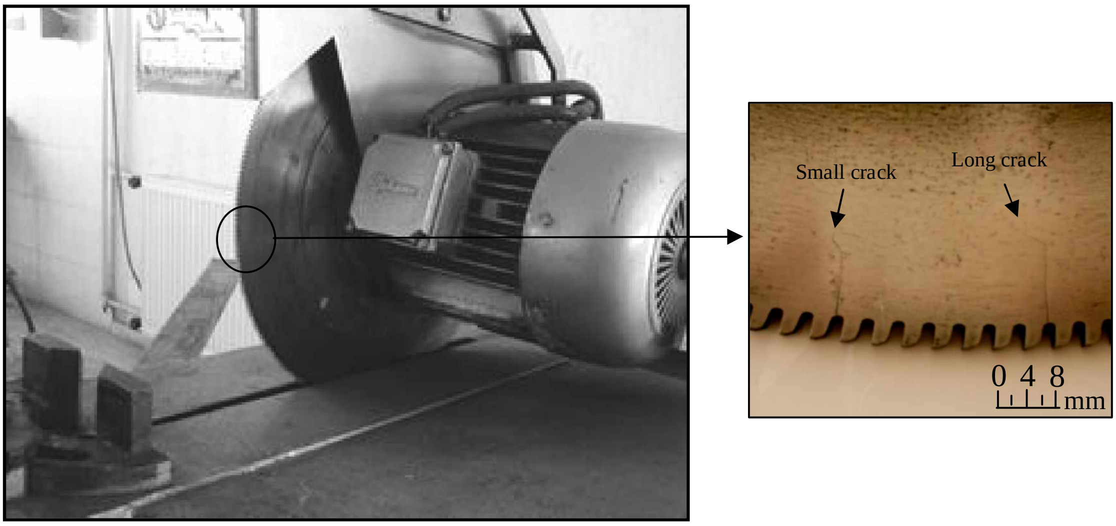


**Figure 1.** Conventional cutting machine and cracked circular saw

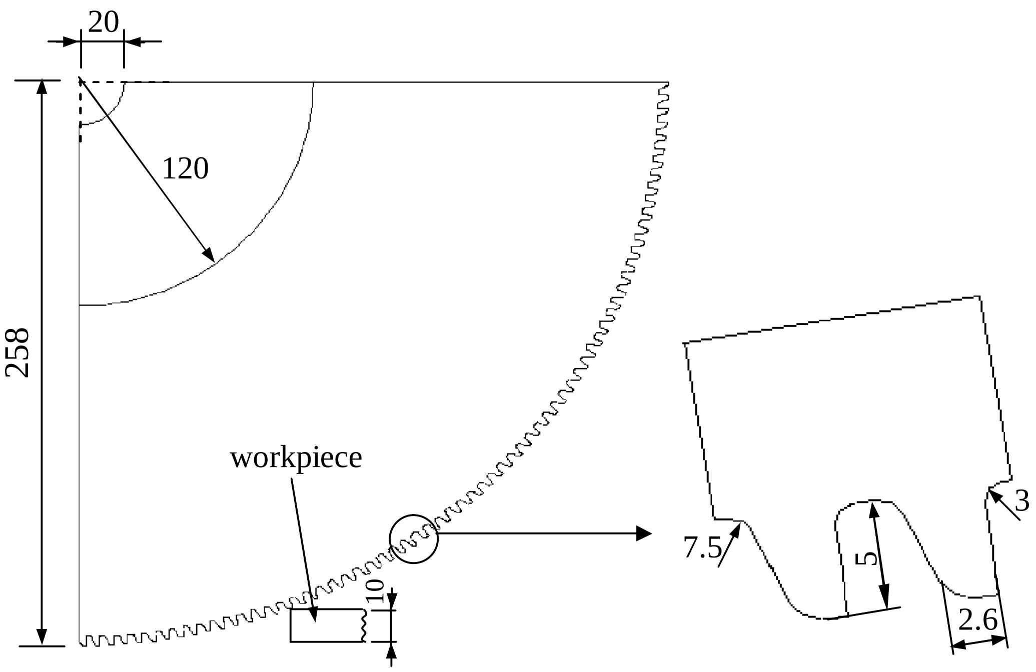


**Figure 2.** Geometrical model of the circular saw with a work piece and geometry of saw teeth.

## 2. EXPERIMENTAL INVESTIGATION

Specimens used in experiments to run mechanical tests, and chemical and metallographic analyses are prepared from the damaged circular saw. Three different mechanical tests namely tensile, hardness and, impact energy tests are applied. An Instron and a Psd 300/150-1 test machines are used for the tensile and impact energy tests respectively. In addition, the hardness measurements are carried out by a MetTest-HT type computer integrated hardness tester.

### 2.1 Chemical Analysis

A sample extracted from the circular saw is applied to spectrometric chemical analysis and the result of it is shown in Table 1. Depending on the material composition in Table 1, it is estimated as tool steel, DIN 17210 which has 60 WCrV 7.[5, 6] According to this standard, Si and Cr must be between 0.55-0.7% and 0.9-1.2% respectively but it is found that Si is 0.202% and Cr is 0.585% in weight. As a result, lower Si element causes oxidation on the circular saw. In addition, lower Cr element in it decreases not only transformation temperature and hardness but also significant amount of wear resistance.

**Table 1.** Chemical analysis of the circular saw material (%wt).

| C | Si | Mo | Mn | Ni | Cu | S | Al | V | Cr |
|---|---|---|---|---|---|---|---|---|---|
| 0.586 | 0.202 | 0.066 | 0.420 | 0.032 | 0.060 | 0.028 | 0.011 | 0.183 | 0.585 |

### 2.2 Microstructure of the Circular Saw

When the microstructure of the circular saw material is analyzed, it is seen that the material is a tempered martensite. Microstructure of the circular saw is given in Figure 3. Usually, martensitic steel is tempered to increase ductility and toughness. The material of the circular saw is thought to be subjected to the quenching at approximately $850^{\circ}C$ which is followed by tempering at approximately $470^{\circ}C$ [5-7]. Grain boundaries are not seen exactly in the microstructure analysis of circular saw due to tempering process.

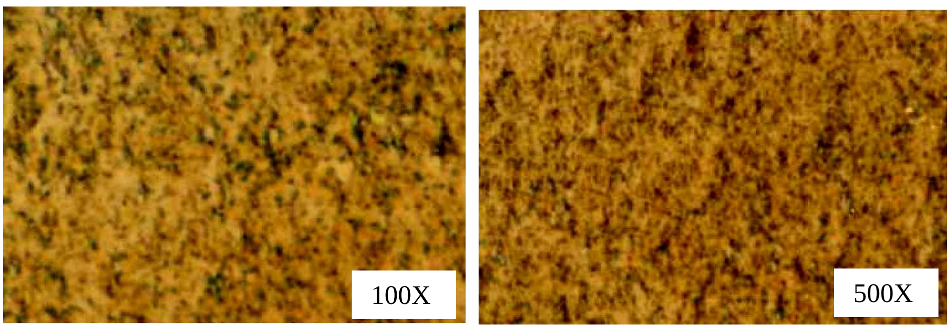


**Figure 3.** Microstructure of the Circular Saw

### 2.3 Mechanical Properties

Results of the mechanical tests are given in Table 2. Using the results of chemical analysis and mechanical tests, the material of circular saw is estimated as medium carbon alloy steel, DIN 17210, with high tensile strength because of quenching and tempering. The hardness is measured as 43 HRC in mid-part of the circular saw where no deformation occurs. On the other hand, severe heating occurred during the cutting process decreases the hardness in tooth root regions where it is measured as 39 HRC.

**Table 2.** Mechanical test results of the circular saw material.

| Elasticity modulus (GPa) | Poisson's ratio | Yield Strength (MPa) | Tensile Strength (MPa) | Total Strain % | Hardness HRC | Impact Energy with notch, (J) |
|---|---|---|---|---|---|---|
| 201 | 0.28 | 640 | 1278 | 15.4 | 43 | 4.1 |

## 3. ANALYSIS

### 3.1 Finite Element Modeling of the Saw

The circular saw is modeled via Franc 2DL finite element software as shown in Fig. 4.[8] Because of symmetry, only one fourth of the saw geometry is drawn to simplify the problem. In addition, isoparametric triangular and quadrilateral elements are used together in the finite element model with 6967 nodes and 2938 elements in solution domain. Also, boundary conditions are constructed around the hole circumference in x and y directions. The material properties (modulus of elasticity and poisson's ratio) of the saw from Table 2 are entered into the program and to investigate stress distribution, 2880 rpm which is measured from the cutting machine and 10 mm constant depth of cut are applied to the model because this circular saw is usually used to cut bars having up to 10 mm thickness. Moreover, forces are constructed in normal and tangential directions, Fig. 4. The maximum force occurs at the first contact point of the tooth. In the analysis, maximum $F_t$ and $F_n$ are taken 2280 and 1845N respectively. These values are calculated using formulas from cutting theory [9,10]. The cutting forces are calculated depending on the depth of cut (10 mm), feed rate (631 mm/min), cutting velocity (2880 rpm) and material properties given in Table 2. The feed rate is measured during a real cutting condition.

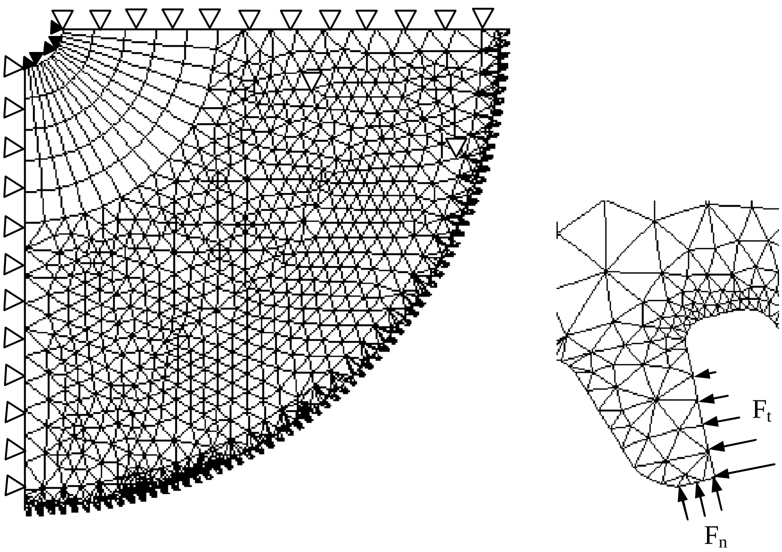


**Figure 4.** Finite element model of the circular saw, its boundary conditions and applied forces to teeth

### 3.2 Fracture Mechanical Analysis

Fatigue crack growth and stress intensity factor (K) are usually investigated in fracture analysis. Because of the two dimensional feature geometry and loading condition, mode I and II are considered in the lineer elastic fracture mechanics analysis by using the finite element method. In addition, the node displacement method is considered to calculate the stress intensity factors. This method is appropriate for numerical solutions based on the finite element method, and is one of the most popular techniques used to calculate the stress intensity factors in numerical studies of fractures [11]. After obtaining finite element solutions for the cracked structure, the displacements of nodes 1-5 (Figure 5) are determined.

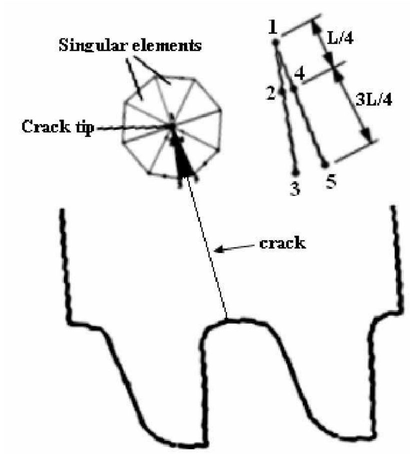


**Figure 5.** The location of the nodes used to calculate the stress intensity factor

The stress intensity factors $K_I$ and $K_{II}$ for opening mode and sliding mode are given by [12]

$$K_I = \frac{G}{\kappa + 1}\sqrt{\frac{2\pi}{L}}\left[4\left(v_2 - v_4\right) + \left(v_5 - v_3\right)\right] \quad (1)$$

$$K_{II} = \frac{G}{\kappa + 1}\sqrt{\frac{2\pi}{L}}\left[4\left(u_2 - u_4\right) + \left(u_5 - u_3\right)\right] \quad (2)$$

where G is the shear modulus and $\kappa$ is defined for plane stress condition as

$$\kappa = \frac{3-\nu}{1+\nu} \quad (3)$$

and L is the element length, $\nu$ is the Poisson's ratio and $u_i$ and $\nu_i$ (i= 2, 3, 4 and 5) are nodal displacement values of the nodes in x ve y directions respectually. In the fracture mechanics, a critical stress intensity factor at the crack tip is used as the failure criteria under static loading. The critical value is called fracture toughness and designeted by $K_{IC}$. The stress intensity factor increases with the increasing crack length. When the crack reaches a certain length, the stress intensity factor reaches to fracture toughness and failure occurs. The fatigue crack propagation behaviour is calculated by the Erdogan-Paris equation [13]

$$\frac{da}{dN} = c \cdot \left(\Delta K\right)^m \quad (4)$$

where $da$ is the increase of the crack length for $dN$ cycles, $\Delta K$ is the range of the stress intensity factor. c and m parameters are constants which depend on material properties. The material parameters having the microstructure given in Fig. 3 and mechanical properties given in Table 2 are given as in the literature $c = 3.31 \cdot (10)^{-17}$, $m = 4.16$ and $K_{IC} = 85$ MPa (m)$^{1/2}$

[14]. The crack propagation of the opening mode is obtained from equation (4). For the mixed mode loading, the stress intensity factor range must be changed with an effective value. It is [11]

$$\Delta K_{eff} = \left(\Delta K_I^4 + \Delta K_{II}^4\right)^{0.25} \tag{5}$$

Fatigue crack growth is assumed to occur either in the plane of maximum shear stress intensity factor range or that of the maximum tensile stress intensity range [11]. The most widely accepted method for the prediction of propagation direction is the maximum principal stress theory. Depending on this theory, the crack propagates in a direction perpendicular to maximum principal stress. The crack propagation direction is calculated from

$$\theta = 2\tan^{-1}\left[\frac{1}{4}\left(\frac{K_I}{K_{II}} \pm \sqrt{\left(\frac{K_I}{K_{II}}\right)^2 + 8}\right)\right] \tag{6}$$

## 4. RESULTS AND DISCUSSIONS

### 4.1 Stress Analysis

The stress analysis is carried out under given load condition with state at plane stress. While cutting forces vary with different factors, the critical region is the same for the circular saw. Figure 6 shows first principal stress distribution of the model. The critical stress concentration takes place at the tooth root region during the cutting process because of cutting forces, and this concentration cause the initiations of fatigue cracks. As can be seen the maximum stress occurred is about 2/3 of the yield strength.

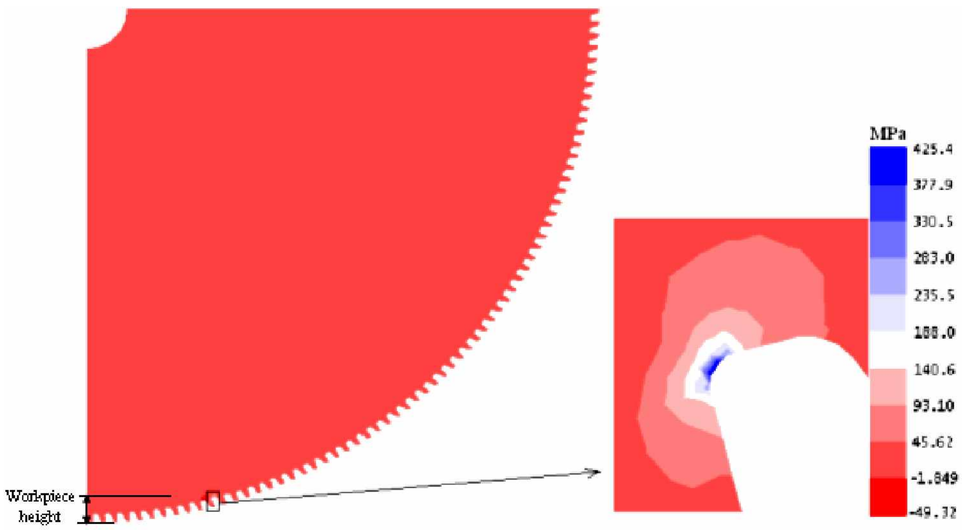


**Figure 6.** Principal stress distribution in the circular saw during the cutting process for 2880 rpm and 10mm dept of cut

### 4.2 Analysis of Fractography

As mentioned above, critical stress concentration occurs in the circular saw especially at the tooth root region under varied forces. Loads which act to the tooth root region are tension forces and they produce crack at this region. Two different cracks close to each other are occurred in the saw analyzed in this study. Fig. 1 shows the damaged area of the saw, and small and long cracks.

As can be seen firstly the fatigue cracks initiate in the disk and grow in the same direction toward to the center of the circular saw. Then, both cracks change their direction to the cutting side. Fig. 7 (a) shows the SEM photograph of the abrupt change of the direction for the long crack and fracture surface of it is seen in Figure 7 (b). In addition, SEM photographs of the small and large cracks are given in Figure 8(a) and (b).

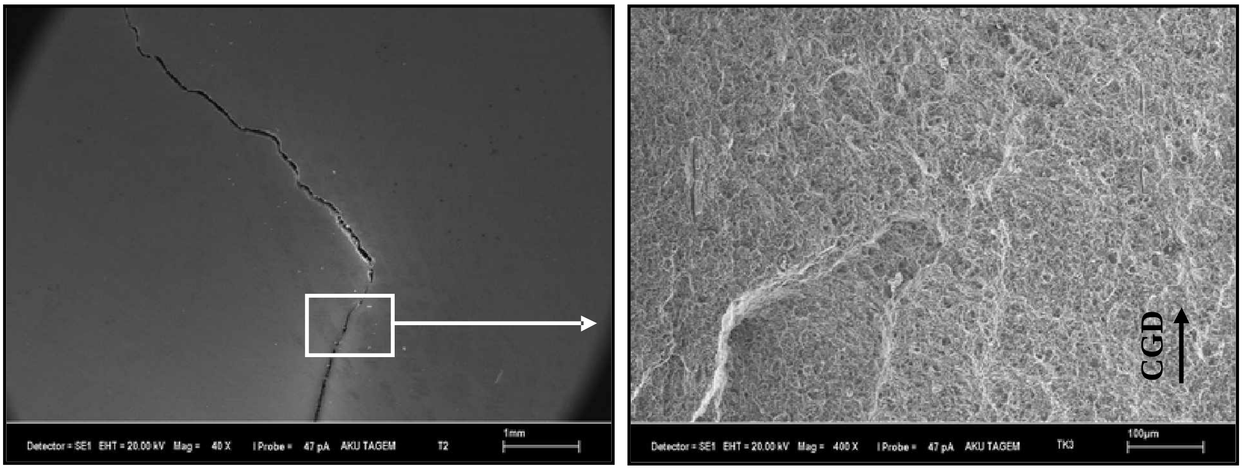


(a) (b)

**Figure 7.** (a) Change of growing direction of the long crack, (b) Fracture surface of the circular saw

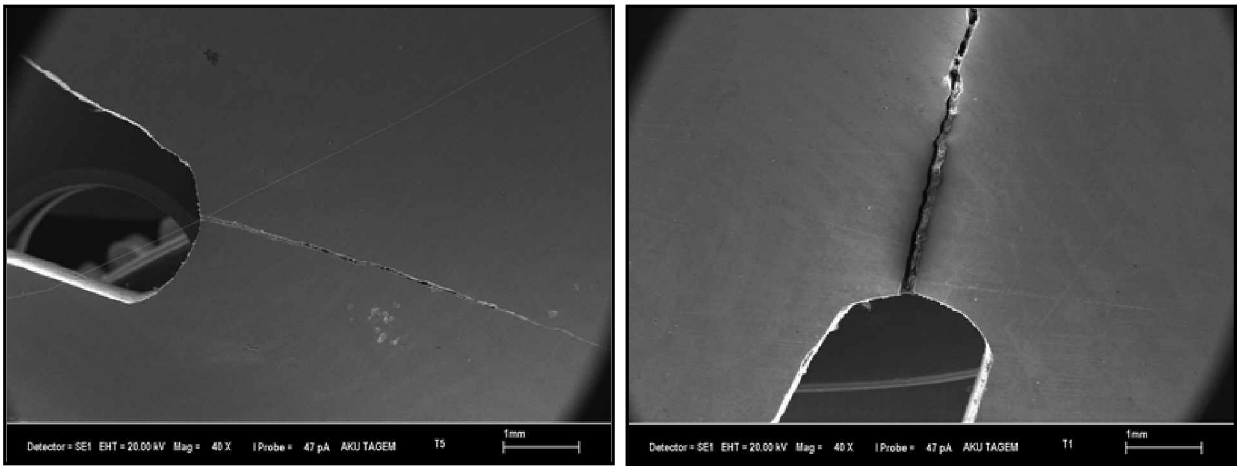


(a) (b)

**Figure 8.** SEM photographs of the (a) small (b) large cracks

### 4.3 Calculation of the Stress Intensity Factors

The stress intensity factors for a given crack and loading configuration are calculated by eq. 1 and 2. When a propagating crack is considered, the stress intensity factors and crack growth direction must be calculated for each increasing crack length. The sign of the $K_{II}$ is important for determining the crack growth direction. Paris and Erdogan [15, 16] have shown that a crack continues to advance in its own plane when it is subjected only to mode I. The presence of positive $K_{II}$ at the crack tip means a turn of the direction to clockwise while negative $K_{II}$ means a counterclockwise turn. In order to calculate the time elapsed for a certain crack length, following procedures are practiced for each loading cycle: Firstly, $K_I$ and $K_{II}$ are calculated for the initial crack length, and then $\Delta K$ is calculated using eq. 5 for the crack configuration. Secondly, d$a$ is determined by the consideration of c and $m$ parameters. This is added to original crack length to obtain the new crack condition by taking the effect of crack front growing direction. The number of the cycle is recorded and procedure is repeated until the desired crack length. In the analysis, variations of $K_I$ and $K_{II}$ are shown in Figure 9 and Figure 10.

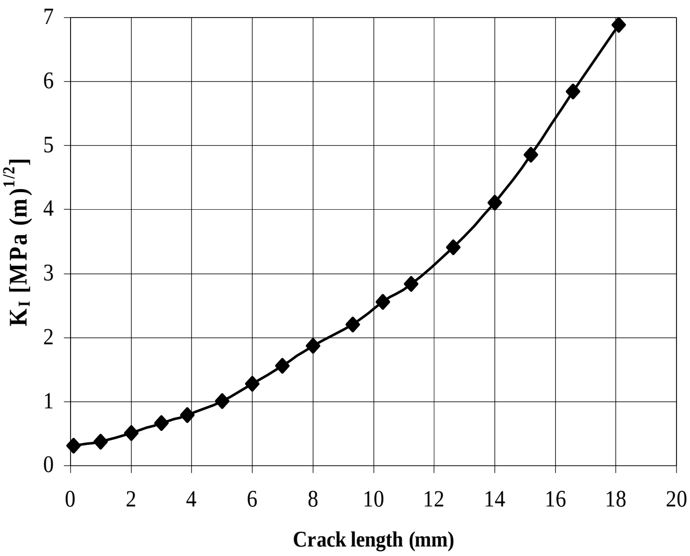


**Figure 9.** Variation of $K_I$ with crack length for long crack

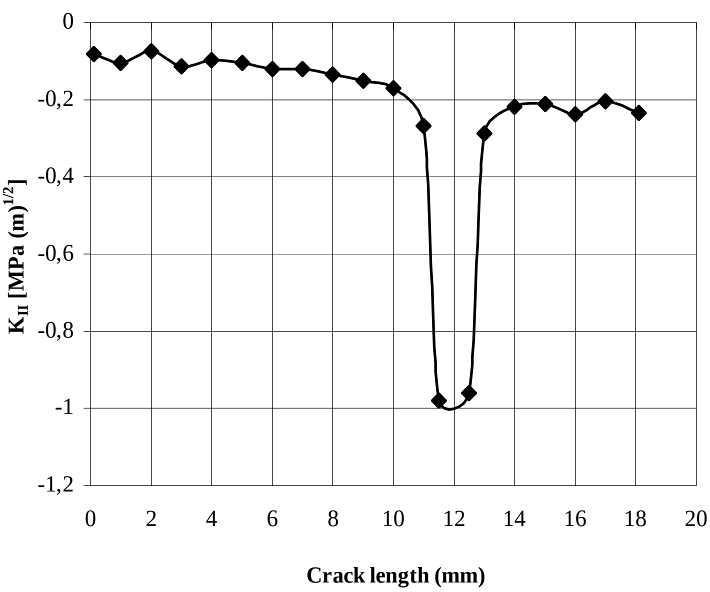


**Figure 10.** Variation of $K_{II}$ with crack length for long crack

The fatigue life of the circular saw is found as 1.02(10^8) cycles after the crack initiation using equation (4) in the numeric analysis. In addition, the fatigue life of the saw is found as 2.327(10^8) cycles before the crack initiation [14]. If this life is compared to the life of the circular saw under working conditions, they are in good agreement. Finally, the total life of the saw is approximately equal to 3.347(10^8) cycles. If the saw is used 2 or 3 hours daily to cut metals, its life will be 966 or 645 days respectively. When they are compared to real applications, these results are reasonable.

The finite element results of the fracture analysis are shown in Figure 11. The crack grows upward and then changes its direction to the cutting side in this numeric investigation as it occurred in the sample disc analysed in this study. Small and long cracks change their directions after a critical point and their lengths are different for each crack. The reason of it might be the initiation site of the crack which is a subject of another study. In numeric analysis, the crack also changes its direction to the same side. In addition, since the saw is investigated as a two-dimensional problem, lateral loads are disregarded. These loads are very small and do not affect the fatigue life.

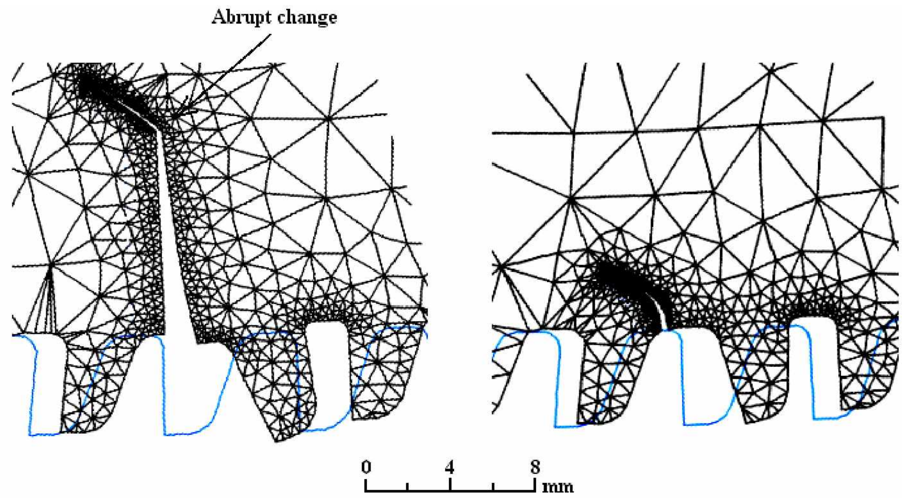


a) b)

**Figure 11.** Finite element model of the cracks a) Long crack c) Small crack

## 5. CONCLUSION

Mechanical and micro-structural properties, and chemical compositions are examined for the circular saw. In addition, fractographic, stress, and fracture analyses are carried out to determine the possible fracture reasons and the fatigue life of the circular saw. Cracks are occurred at the tooth root region where the stress concentration is maximum during the cutting process and close to each other in the circular saw. Both cracks grow toward to the center of the circular saw. In addition, the cracks shift their directions to the cutting side of the saw after a point which is a critical condition for the saw. Experimental and numerical fatigue crack propagations are in good agreement. The value of $K_{II}$ is usually used to determine the crack direction. $K_I$ is also determined in numeric analysis. As a result of the numerical fracture analysis, the fatigue life is estimated as 1.02(10^8) cycles after the crack initiation. The total life of the saw is approximately equal to 3.347(10^8) cycles. This result is reasonable real applications. Finally, undesired shock forces during the cutting process might be effective for fracture in addition to feed rate, revolution speed of the saw, types of material being sawed, depth of cut, and material defects of the circular saw.

## ACKNOWLEDGEMENTS

The authors gratefully acknowledge the support of the Research Foundation of Afyon Kocatepe University in this study.

## REFERENCES

**1.** Andersson, C., “Bandsawing Part III: Stress Analysis of Saw Tooth Microgeometry”, **International Journal of Machine Tools & Manufacture**, Vol 41, p 255-263, 2001.
**2.** Nordström, J., Bergström, J., “Wear Testing of Saw Teeth in Timber Cutting”, **Wear**, Vol 250, p 19–27, 2001.
**3.** Fukaura, K., Yokoyama, Y., Yokoi, D., Tsujii, N., Ono, K., “Fatigue of Cold-Work Tool Steels: Effect of Heat Treatment and Carbide Morphology on Fatigue Crack Formation, Life, and Fracture Surface Observation”, **Metallurgical and Materials Transactions A**, Vol 35(04A), p 1289, 2004.
**4.** Yesildal, R., Sen, S., Kaymaz, I., “Fatigue Behaviour of X40CrMoV 51 at High Temperatures”, **Journal of Materials Engineering and performance**, Vol 12(02), p 215, 2003.
**5.** Heat Treaters Guide: Practices and procedures for irons and steels, ASM International, p 313-340 and 889, 1995.
**6.** Topbaş, M.A., Çelik El Kitabı ve Isıl İşlem. October Press, Istanbul, (in Turkish), 1998.
**7.** ASM Specialty Handbook; Carbon and Alloy Steels, **ASM International**, p 19, 1996.
**8.** Franc2D, User’s Manual, Available from <www.cfg.cornell.edu >.
**9.** Akkurt,M., “Talaş kaldırma metotları ve takım tezgahları (Chip removing methods and tool machining)”, **Birsen publishing**, Istanbul, Turkey, 1996.
**10.** Bootroyd, G., “Fundamentals of Metals Machining and Machine Tools”, **Mcgraw Hill**, United State of America, Newyork, 1989.
**11.** Aslantaş, K., Taşgetiren, S., “Modelling of Spall Formation in a Plate Made of Austempered Ductile Iron Having a Subsurface-Edge Crack”, **Computational Materials Science**, Vol 29, p 29-36, 2004.
**12.** Tan, C.L., Gao, Y.L., “Treatment of Bimaterial Interface Crack Problems Using the Boundary Element Method”, **Eng. Fract. Mechanics**, Vol 36(6), p 919-932, 1990.
**13.** Ergun, E., Aslantaş, K., Taşgetiren, S., Topçu, M., “Fracture Analysis of Resistance Welded L-Shaped and Straight Sheets”, **Materials and Design**, Vol 27, p 2-9, 2006.
**14.** Glodez, S., Sraml, M., Kramberger, J., “A Computational Model for Determination of Service Life of Gears”, **International Journal of Fatigue**, Vol 24, p 1013-1020, 2002.
**15.** Paris, P.C., Erdoğan, F., “A Critical Analysis of Crack Propagation Laws”, **J. Basic Eng.**, Vol 85, p 528-534, 1961.
**16.** Erdoğan, F. Sih, G.C., “On the Crack Extension in Plates Under Plane Loading and Transverse Shear”, **J. Basic Eng.**, Vol 85, p 519-527, 1963.